Title

Factors driving availability of COVID-19 convalescent plasma: Insights from a demand, production, and supply model.

Journal

Transfusion, 61(5)

Authors

Russell, W

Grebe, Eduard

Custer, Brian

Publication Date

2021-05-01

DOI

10.1111/trf.16317

Peer reviewed

Received: 25 October 2020 | Revised: 4 January 2021 | Accepted: 4 January 2021

DOI: 10.1111/trf.16317

BRIEF REPORT

TRANSFUSION

Factors driving availability of COVID-19 convalescent plasma: Insights from a demand, production, and supply model

W. Alton Russell[1,2†] | **Eduard Grebe**[1,3†] | **Brian Custer**[1,3]

[1]Vitalant Research Institute, San Francisco, California, USA

[2]Department of Management Science and Engineering, Stanford University, Stanford, California, USA

[3]Department of Laboratory Medicine, University of California San Francisco, San Francisco, California, USA

Correspondence
Eduard Grebe, Vitalant Research Institute, 270 Masonic Avenue, San Francisco, CA 94118.
Email: egrebe@vitalant.org

Abstract

Background: COVID-19 Convalescent Plasma (CCP) is a promising treatment for COVID-19. Blood collectors have rapidly scaled up collection and distribution programs.

Methods: We developed a detailed simulation model of CCP donor recruitment, collection, production, and distribution processes. We ran our model using varying epidemic trajectories from 11 U.S. states and with key input parameters drawn from wide ranges of plausible values to identify key drivers of ability to scale collections capacity and meet demand for CCP.

Results: Utilization of available CCP collections capacity followed increases in COVID-19 hospital discharges with a lag. Utilization never exceeded 75% of available capacity in most simulations. Demand was met for most of the simulation period in most simulations, but a substantial portion of demand went unmet during early, sharp increases in hospitalizations. For epidemic trajectories that included multiple epidemic peaks, second wave demand could generally be met due to stockpiles established during the decline from an earlier peak. Apheresis machine capacity (number of machines) and probability that COVID-19 recovered individuals are willing to donate were the most important supply-side drivers of ability to meet demand. Recruitment capacity was important in states with early peaks.

Conclusions: Epidemic trajectory was the most important determinant of ability to meet demand for CCP, although our simulations revealed several contributing operational drivers of CCP program success.

KEYWORDS

blood products, convalescent plasma, COVID-19, SARS-CoV-2, simulation modeling

1 | INTRODUCTION

The novel coronavirus SARS-CoV-2 has fueled a global pandemic, with more than 37 million confirmed COVID-19 cases and 1 million deaths as of October 12, 2020.[1] Transfusion of convalescent plasma from recovered individuals with a mature antibody response has been successfully used for post-exposure prophylaxis and treatment during other disease outbreaks, including two other coronaviruses: severe acute respiratory syndrome (SARS-1) and Middle East respiratory syndrome (MERS).[2,3] In response to the SARS-CoV-2 pandemic, blood collectors rapidly established COVID-19 Convalescent Plasma (CCP) collection, processing, and distribution programs during the

† These authors contributed equally to this work.

first half of 2020. Available evidence suggests that CCP is safe and may be an effective treatment, although some smaller trials did not find evidence of efficacy, and results from large randomized controlled trials are pending.[4–7] Because CCP is a new and unique blood product, limited data are available regarding the operational challenges of CCP collection and distribution programs during an epidemic.

Using data from a nonprofit organization that collects approximately 14% of the US blood supply, we developed a simulation model of CCP donor recruitment, donation collection, testing, and distribution processes. In this paper, we use our simulation to evaluate how epidemic trajectory, donor recruitment and retention, collections capacity, and demand impact ability to meet competing priorities of current clinical demand and stockpiling CCP for future use in 11 different U.S. states. Our aim was not to replicate the initial history of CCP collections in each state but rather to analyze and gain insights into the diverse set of drivers of a successful CCP program.

2 | METHODS

We ran our simulation for 11 epidemic trajectories while varying parameters related to CCP donor recruitment and return, collections capacity, and demand. Epidemic trajectories were based on calibrated state-level SEIR epidemic models developed and published by 'COVID Act Now'.[8] We included 10 states with the highest cumulative per-capita COVID-19 hospitalization rate as of August 31, 2020 (New Jersey, New York, Massachusetts, Illinois, Louisiana, Connecticut, Indiana, Mississippi, Virginia, and Maryland) and California, which had the highest overall number of COVID-19 hospitalizations during this period. We excluded Washington D.C. despite having the highest estimated per-capita hospitalization rate because it had fewer than 10,000 total hospitalizations.

For each state, we estimated daily hospital admissions and discharges from three reported outcomes in the COVID Act Now state-level models (hospital beds required, deaths, and infections by day) using a method described in the appendix. We ran 10,000 simulations of a 200-day period beginning on the date of the first discharge of a COVID-19 patient and calculated two daily outcomes: (1) the percent of CCP collection capacity utilized and (2) the percent of CCP demand unmet. In each simulation, we sampled seven input parameters related to donor recruitment and return, collections capacity, and CCP demand using uniform distributions.

Our simulation model consisted of two linked components: (1) a microsimulation of the donor recruitment, return, collections, and CCP screening processes and outputs a number of usable units collected by day and (2) a production model that accounts for production lag, demand, distribution, and inventory.

2.1 | Donor recruitment and return

In the simulation, potential CCP donors (agents) entered the model at discharge from hospital and become eligible for CCP donation 14 days later. Across simulations, we varied the probability a recovered individual would be willing to donate CCP from 10% to 90%, and we varied capacity for new donor recruitment from 0.2 to 2 new donors each day per apheresis machine. Willing donors who were recruited each day entered the donor pool. Each day, donors in the pool were selected randomly and scheduled for donations, subject to a collection capacity. Scheduled donations could be incomplete due to donor deferral for other reasons (2% probability) or failed or incomplete donation (1% probability). Completed donations could be removed from the CCP supply due to testing positive for disease markers (0.2% probability), not meeting the SARS-CoV-2 antibody release criterion (8% probability), or testing positive for HLA antibodies (9% probability for female donors). These probabilities were based on data from the first seven months of the CCP program. CCP donors could return for additional donation as soon as 7 days later, a policy many U.S. blood centers implemented in consultation with the FDA as a modification to the 28-day interval required for standard plasmapheresis donation.[9] Due to concern over potential antibody waning,[10] which may affect neutralizing antibody titers and the product's clinical effectiveness, donors in the model became ineligible for CCP donation 180 days after discharge. For each donor, we sampled the minimum number of days until a subsequent donation attempt from an empirical distribution fit to the CCP donation data. We developed separate distributions for time to return for the donor's second, third, and fourth-or-greater donation, respectively, based on differences in return donation propensity observed in the data (Figure S1). We assumed that donors who do not return by 130 days would never return: 57%, 31%, and 11% of donors never returned for a second, third, or fourth-or-greater donation, respectively.

2.2 | Capacity

In each state, we varied the per capita number of apheresis machines from 4 to 55 per million residents. We assumed that each machine could support on average 3.5 plasma collection procedures per day. Due to demand for other apheresis products, we assumed that only 50% of machines would be available for CCP collections each

day. We based the range of per-capita apheresis machines on the rates for three states for which we had data: Colorado (eight machines per million residents), South Dakota (34 machines per million residents), and North Dakota (55 machines per million residents).

2.3 | Demand

We calculated daily CCP demand from the estimated daily hospital admissions and three parameters: the probability each hospitalized COVID-19 patient requires CCP (varied from 10% to 45% of patients), the number of CCP units required per patient (varied from 1.5 to 4 units), and the average delay from admission to receiving CCP transfusion (varied from 1 to 5 days). In the simulation, the daily number of CCP units produced and any existing inventory was used to meet demand. If the available CCP exceeded demand, it was added to inventory and available to meet future demand.

2.4 | Sensitivity analysis

For sensitivity analysis, we performed a separate set of simulations in which we also varied donor return. To do so, we fit an exponential distribution to the probability a donor returns by t days from their last donation of the form

$$P(t) = \begin{cases} K\left(1 - e^{-\lambda(t-t_0)}\right), & \text{if } t \geq t_0 \\ 0, & \text{otherwise} \end{cases}$$

We set t_0 (the minimal return time) to 7 days in line with current practice, and fit λ (the exponential rate parameter) and K (the asymptote limiting donor return) to the empiric donor return data using maximum likelihood estimation. As before, we used separate distributions for the second, third, and fourth-or-greater donations. To vary return time, we added a scaling factor s as follows:

$$P(t) = \begin{cases} sK\left(1 - e^{-s\lambda(t-t_0)}\right), & \text{if } t \geq t_0 \\ 0, & \text{otherwise} \end{cases}$$

This distribution leads to greater return when $s > 1$ and less donor return when $s < 1$. In sensitivity analysis, we varied s from 0.5 to 2.25 only in the distribution for second donations.

To assess the sensitivity of the total percent demand unmet to each parameter in each state, we regressed each parameter on the outcome using locally estimated scatterplot smoothing (LOESS), a non-parametric regression model that produces smooth curves. We then predicted the outcome at the 1st, 25th, 50th, 75th, and 99th percentile of each input. We assessed the degree to which the predicted outcome changed depending on the quantile of parameter used to predict it, an indication of how sensitive the ability to meet demand was to the parameter (or how important the parameter was). We developed an easy-to-use web-based modeling tool, available at https://vitalantri.shinyapps.io/ccp_model. All code is open source and publicly available.[11]

3 | RESULTS

Across states, increases in collection capacity utilization lagged behind increases in COVID-19 patient discharge by 2 weeks, reflecting the delay in donor eligibility (Figure 1). In periods when discharges fell sharply, collections capacity utilization fell more gradually. In more than 50% of simulations across all states, percent collection capacity utilized never exceeded 75% of available machine time, indicating that fully utilizing available collection capacity may be an important challenge.

In most simulations, states met most of the demand during most of the period despite relatively low capacity utilization (Figure 2). Demand was more likely to go unmet during early increases in hospitalizations, particularly in states with very steep hospitalization increases (e.g., New York). Most of the demand was met in most simulation for states with more gradual increases (e.g., Virginia and California). In states with two epidemic peaks (e.g., Louisiana, Indiana) demand was mostly met during the second wave using inventory stockpiled during the downswing from the first peak (Figure S2 shows inventory over time by state).

The sensitivity of percent demand unmet to uncertain parameters is plotted in Figure 3 for four states and in Figure S3 for the other states. Apheresis machine capacity was a strong determinant of the percent demand unmet. Given that we assumed recruitment capacity was proportional to the number of machines, some of that benefit could be attributed to increased donor recruitment. Both the fraction of hospitalized patients requiring CCP and the number of units transfused per patient were more important parameters than the delay from admission to CCP administration. The scale multiplier on donor return did not substantially impact ability to meet demand. In most states, the probability COVID-19 recovered individuals were willing to donate was the most important donor-related parameter. However, the daily donor recruitment capacity was more important in

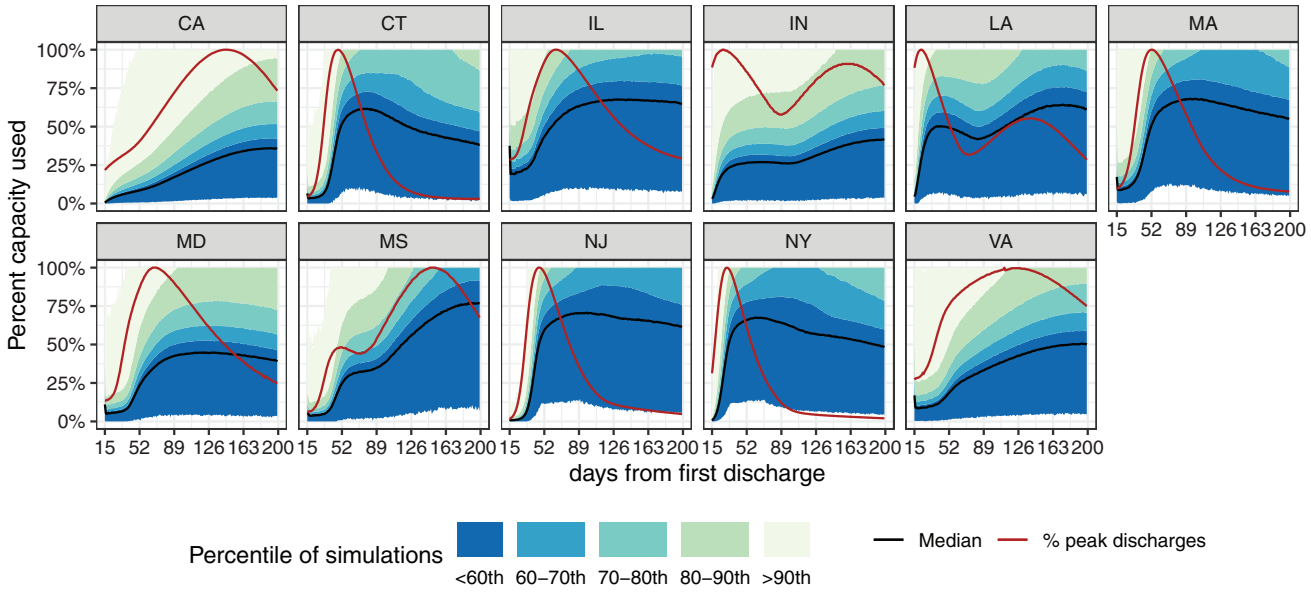

FIGURE 1 Percent of available collections capacity used each day of the simulation period by state. The median of the percent collections capacity used across 10,000 simulations is shown by a black line. The epidemic trajectory is indicated by a red line that shows how many patients were discharged each day relative to the number discharged at the epidemic peak for each state. The 60th, 70th, 80th, and 90th percentiles of the percent collections capacity used are also indicated for each day of the simulation period by the boundaries between colored regions [Color figure can be viewed at wileyonlinelibrary.com]

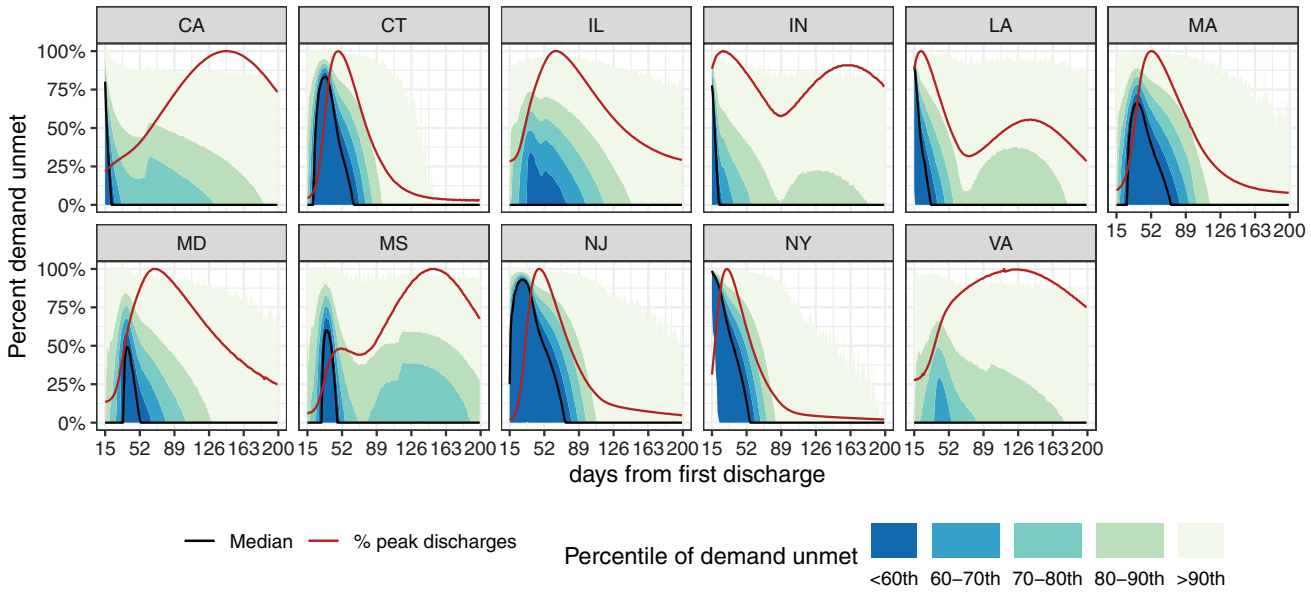

FIGURE 2 Percent of CCP demand unmet each day of the simulation period by state. The median of the percent demand unmet across 10,000 simulations is shown by a black line. The epidemic trajectory is indicated by a red line that shows how many patients were discharged each day relative to the number discharged at the epidemic peak for each state. The 60th, 70th, 80th, and 90th percentiles of the percent demand unmet are also indicated for each day of the simulation period by the boundaries between colored regions [Color figure can be viewed at wileyonlinelibrary.com]

New York and New Jersey. Both these states experienced very early, steep epidemic trajectories that yielded many potential CCP donors, which may explain why capacity to recruit was a more important parameter than willingness to donate. In a scenario analysis, we found that if inventory were shared across all states (as it is in reality), the median percent of demand unmet over the simulation period dropped from 27% to 16% (Figure S4).

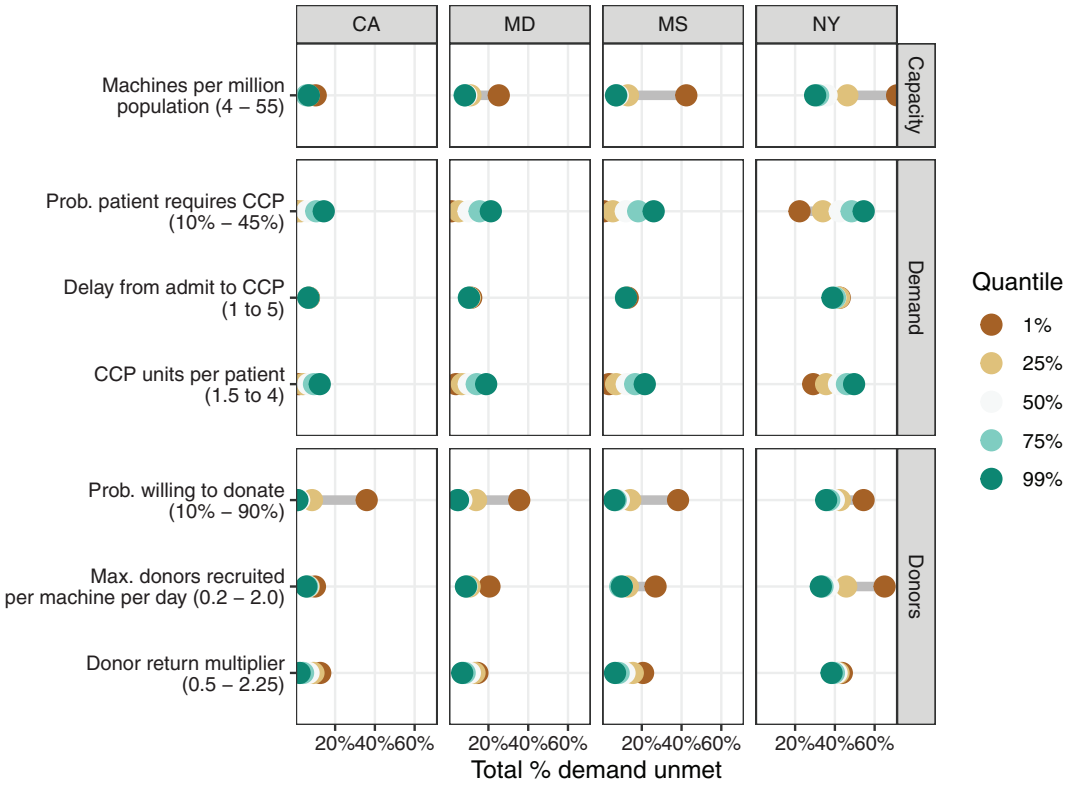

FIGURE 3 Sensitivity of the total percent demand unmet over the simulation period to changes in seven parameters. Regression was used to estimate how changing a single parameter from the 1st to 99th quantile of the values it took across the 10,000 simulations would change the total percent demand unmet. Greater distance between plotted points indicates that ability to meet demand was more sensitive to changes in the indicated parameter. Four states selected to represent a diverse set of epidemic trajectories are shown here; the remaining seven states are shown in Figure S2 [Color figure can be viewed at wileyonlinelibrary.com]

4 | DISCUSSION

Our analysis showed that epidemic trajectory was a key driver of ability to meet CCP demand. While donor willingness to return was not a driver of outcomes in our simulations, the percentage of donors deferred or unwilling to return increased to very high levels over the simulation period in all states (Figure S5), indicating that it could be important over a longer time horizon and when insufficient CCP donors are recruited during initial epidemic peaks.

Unexpectedly, our analysis suggests that blood centers may struggle to fully utilize capacity and meet demand for CCP collections, particularly during rapid increases in the epidemic. In periods when demand is not quickly growing, blood centers can likely meet demand even when capacity utilization is fairly low. While ability to meet demand was sensitive to several parameters, epidemic trajectory was most important (Figure S6). Our simulations also demonstrated that having inventory on hand before an increase in demand greatly increased ability to meet demand.

The evidence base for CCP, and both operational practices and regulatory policies are evolving rapidly. Our simulations were largely informed by the experience of one large blood collector, which may differ from that of other blood collectors. We also assumed donors would not return after 180 days due to uncertainty around antibody waning. This assumption had minimal impact on our analysis because we only modeled a 200-day period starting with the first COVID-19 patient discharge in each state. However, antibody waning and longer-term donor return behavior are increasingly important considerations as the pandemic progresses and in the context of regulatory requirements to label CCP products as high or low titer. We further assumed an early start to and stable efforts in recruitment and collection, rather than a gradual ramp-up. Despite these limitations, our analysis reveals key drivers of the ability to utilize capacity and meet demand for CCP during an epidemic.

ACKNOWLEDGMENTS

The authors thank the many Vitalant team members who provided expertise and data that informed model development. The authors also thank the COVID Act Now team for developing the epidemic model used for this analysis (http://covidactnow.org/). This work was funded by Vitalant.

CONFLICT OF INTEREST

W.A.R. and B.C. have provided consulting services outside the submitted work for Terumo BCT, a manufacturer of apheresis equipment.

ETHICS/CONSENT

No human subjects or identifiable data were involved in this analysis.

DATA AND MATERIALS

We have shared all data in a public repository except for the individual donor return data.

CODE AVAILABILITY

We have shared all code in a public repository (https://doi.org/10.5281/zenodo.4082755).

AUTHORS' CONTRIBUTIONS

All authors developed the research question and methods and critically reviewed the manuscript. All authors identified sources and obtained data for the model. E.G. and W.A.R. conducted the analysis (E.G. led development of the donor microsimulation and W.A.R. led development of the policy analysis) and wrote the manuscript. B.C. provided critical review of the manuscript.

ORCID

W. Alton Russell https://orcid.org/0000-0003-1780-4470
Eduard Grebe https://orcid.org/0000-0001-7046-7245
Brian Custer https://orcid.org/0000-0001-6251-366X

REFERENCES

1. World Health Organization. WHO Coronavirus Disease (COVID-19) Dashboard. 2020. [cited 2020 Oct 12]. Available from: https://covid19.who.int/.
2. Ko JH, Seok H, Cho SY, Eun Ha Y, Baek JY, Kim SH, et al. Challenges of convalescent plasma infusion therapy in middle east respiratory coronavirus infection: A single centre experience. Antivir Ther. 2018;23(7):617–22. https://doi.org/10.3851/IMP3243.
3. Yeh KM, Chiueh TS, Siu LK, Lin JC, Chan PKS, Peng MY, et al. Experience of using convalescent plasma for severe acute respiratory syndrome among healthcare workers in a Taiwan hospital. J Antimicrob Chemother. 2005;56(5):919–22. https://doi.org/10.1093/jac/dki346.
4. Joyner MJ, Bruno KA, Klassen SA, Kunze KL, Johnson PW, Lesser ER, et al. Safety update: COVID-19 convalescent plasma in 20,000 hospitalized patients. Mayo Clin Proc. 2020;95(9):1888–97. https://doi.org/10.1016/j.mayocp.2020.06.028.
5. Klassen SA, Senefeld JW, Johnson PW, Carter RE, Wiggins CC, Shoham S, et al. Evidence favoring the efficacy of convalescent plasma for COVID-19 therapy. medRxiv. 2020;2020.07.29.20162917. https://doi.org/10.1101/2020.07.29.20162917.
6. Simonovich VA, Burgos Pratx LD, Scibona P, Beruto MV, Vallone MG, Vázquez C, et al. A randomized trial of convalescent plasma in COVID-19 severe pneumonia. N Engl J Med. 2020. https://doi.org/10.1056/NEJMoa2031304.
7. Agarwal A, Mukherjee A, Kumar G, Chatterjee P, Bhatnagar T, Malhotra P. Convalescent plasma in the management of moderate COVID-19 in adults in India: Open label phase II multicentre randomised controlled trial (PLACID trial). BMJ. 2020;371:m3939. https://doi.org/10.1136/bmj.m3939.
8. COVID Act Now. COVID Act Now API 2020. [cited 2020 Sept 8]. Available from: https://covidactnow.org/resources#api.
9. Budhai A, Wu AA, Hall L, Strauss D, Paradiso S, Alberigo J, et al. How did we rapidly implement a convalescent plasma program? Transfusion. 2020;60(7):1348–55. https://doi.org/10.1111/trf.15910.
10. Perreault J, Tremblay T, Fournier M-J, Drouin M, Beaudoin-Bussières G, Prévost J, et al. Waning of SARS-CoV-2 RBD antibodies in longitudinal convalescent plasma samples within four months after symptom onset. Blood. 2020;136(22):2588–91. https://doi.org/10.1182/blood.2020008367.
11. Grebe E, Russell WA, Custer B. COVID-19 convalescent plasma model. Zenodo. 2020. https://doi.org/10.5281/zenodo.4082755.

SUPPORTING INFORMATION

Additional supporting information may be found online in the Supporting Information section at the end of this article.

How to cite this article: Russell WA, Grebe E, Custer B. Factors driving availability of COVID-19 convalescent plasma: Insights from a demand, production, and supply model. *Transfusion*. 2021; 61:1370–1376. https://doi.org/10.1111/trf.16317

APPENDIX

Eduard Grebe, W. Alton Russell, Brian Custer

PROCEDURE FOR ESTIMATING DAILY HOSPITAL ADMISSIONS AND DISCHARGES FROM COVID ACT NOW MODEL OUTPUT

Our microsimulation model of the donor recruitment and collection process relies on a virtual cohort of potential CCP donors. At each time step, new agents are created equal to the estimated number of individuals discharged from hospital after recovery from severe COVID-19. Our production and supply model relies on the estimated number of new ICU admissions by day. We estimated the number of discharges from hospital and admissions to ICU from the output of state-level SEIR epidemic models published by 'COVID Act Now'.

The published 'COVID Act Now' model output time series do not include new recoveries or hospital

admissions and discharges. However, these can be estimated from the variables that are provided:

- cumulativeDeaths (cD_t)
- cumulativeInfected (cI_t)
- currentInfected (I_t)
- currentSusceptible (S_t)
- currentExposed (E_t)
- hospitalBedsRequired (H_t)

Given the following identities:

$$\begin{aligned} I_{t+1} &= I_t + \text{infections}_t - \text{recoveries}_t - \text{deaths}_t \\ cI_{t+1} &= cI_t + \text{infections}_t \\ cD_{t+1} &= cD_t + \text{deaths}_t \end{aligned}$$

we can obtain the number of recoveries at each timestep by rearranging and substituting:

$$\begin{aligned} \text{recoveries}_t &= I_t - I_{t+1} + \text{infections}_t - \text{deaths}_t \\ &= I_t - I_{t+1} + [cI_{t+1} - cI_t] - [cD_{t+1} - cD_t] \\ &= I_t - I_{t+1} + cI_{t+1} - cI_t - cD_{t+1} + cD_t \end{aligned}$$

By assuming that the proportion of recoveries that represent discharges from hospital is equal to the proportion of infected individuals that are hospitalized, we can obtain the number of discharges from hospital by day:

$$\text{discharges}_t = \text{recoveries}_t \cdot \frac{H_t}{I_t}$$

Once we have estimated the number of discharges by day, we are able to obtain the number of new hospital admissions by day:

$$\begin{aligned} H_{t+1} &= H_t - \text{discharges}_t - \text{deaths}_t + \text{admissions}_t \\ \text{admissions}_t &= H_{t+1} - H_t + \text{discharges}_t + \text{deaths}_t \end{aligned}$$

To estimate the number of ICU admissions by day, we assumed that:

- a certain proportion of patients hospitalized with COVID-19 never require critical care
- a certain proportion are admitted directly to the ICU (p_d)
- a certain proportion are stepped up to critical care (p_s) after a certain time (τ) in standard care

We assumed $p_d = 0.04$ and $p_s = 0.12$, which are similar to observed values in hospitalization data from Québec, Canada (based on data in the "MED-ECHO" system owned by the Ministère de la Santé et des Services sociaux). The distribution of times from admission to care step-up has a long tail, but the vast majority of patients who are stepped up to critical care are admitted to the ICU in the first few days after hospitalization, with a median delay of 2 days ($\tau = 2$). For the purposes of estimating ICU admissions by day we used the median value.

$$\text{ICU admissions}_t = p_d \cdot \text{admissions}_t + p_s \cdot \text{admissions}_{t-\tau}$$